Biomedicine & Pharmacotherapy 170 (2024) 115850

Contents lists available at ScienceDirect

Biomedicine & Pharmacotherapy

journal homepage: www.elsevier.com/locate/biopha

KUS121, a VCP modulator, has an ameliorating effect on acute and chronic heart failure without calcium loading via maintenance of intracellular ATP levels

Shuhei Tsuji [a,1], Chiharu Otani [a,1], Takahiro Horie [a], Shin Watanabe [a], Osamu Baba [a,b], Naoya Sowa [c], Yuya Ide [a], Asami Kashiwa [a], Takeru Makiyama [a], Hirohiko Imai [f], Yasuhiro Nakashima [a], Tomohiro Yamasaki [a], Sijia Xu [a], Kazuki Matsushita [a], Keita Suzuki [d], Fuquan Zou [a], Eitaro Kume [e], Koji Hasegawa [b], Takeshi Kimura [a], Akira Kakizuka [g,*], Koh Ono [a,*]

[a] Department of Cardiovascular Medicine, Kyoto University Graduate School of Medicine, Kyoto 606-8507, Japan
[b] Preemptive Medicine and Lifestyle Disease Research Center, Kyoto University Hospital Kyoto, 606-8507, Japan
[c] Division of Translational Research, National Hospital Organization, Kyoto Medical Center, 1-1 Fukakusa Mukaihata-cho, Fushimi-ku, Kyoto 612-8555, Japan
[d] Department of Neurosurgery, Kyoto University Graduate School of Medicine, Kyoto 606-8507, Japan
[e] Department of Pediatrics, Kyoto University Graduate School of Medicine, Kyoto 606-8507, Japan
[f] Department of Systems Science, Graduate School of Informatics, Kyoto University, Kyoto 606-8501, Japan
[g] Laboratory of Functional Biology, Kyoto University Graduate School of Biostudies and Solution Oriented Research for Science and Technology, Kyoto 606-8501, Japan

ARTICLE INFO

Keywords:
Heart failure
ATP
KUS121
Therapeutic agent

ABSTRACT

Aims: As heart failure (HF) progresses, ATP levels in myocardial cells decrease, and myocardial contractility also decreases. Inotropic drugs improve myocardial contractility but increase ATP consumption, leading to poor prognosis. Kyoto University Substance 121 (KUS121) is known to selectively inhibit the ATPase activity of valosin-containing protein, maintain cellular ATP levels, and manifest cytoprotective effects in several pathological conditions. The aim of this study is to determine the therapeutic effect of KUS121 on HF models.

Methods and results: Cultured cell, mouse, and canine models of HF were used to examine the therapeutic effects of KUS121. The mechanism of action of KUS121 was also examined. Administration of KUS121 to a transverse aortic constriction (TAC)-induced mouse model of HF rapidly improved the left ventricular ejection fraction and improved the creatine phosphate/ATP ratio. In a canine model of high frequency-paced HF, administration of KUS121 also improved left ventricular contractility and decreased left ventricular end-diastolic pressure without increasing the heart rate. Long-term administration of KUS121 to a TAC-induced mouse model of HF suppressed cardiac hypertrophy and fibrosis. In H9C2 cells, KUS121 reduced ER stress. Finally, in experiments using primary cultured cardiomyocytes, KUS121 improved contractility and diastolic capacity without changing peak Ca^{2+} levels or contraction time. These effects were not accompanied by an increase in cyclic adenosine monophosphate or phosphorylation of phospholamban and ryanodine receptors.

Conclusions: KUS121 ameliorated HF by a mechanism totally different from that of conventional catecholamines. We propose that KUS121 is a promising new option for the treatment of HF.

1. Introduction

Heart failure (HF) is a debilitating disease that has a major clinical and economic impact on people around the world, and it is increasingly prevalent with the increase of the aging population [1]. Despite significant advances in diagnosis and treatment over the past 20 years, patients with HF still have a poor long-term prognosis. Catecholamines, e.g. isoproterenol or other β-agonists, can improve cardiac output, but these drugs have serious adverse effects on the heart, such as increasing the heart rate, increasing cardiac oxygen consumption, and often exacerbating heart failure. Thus, novel therapeutic targets are urgently needed to improve heart function in patients with heart failure, as well

* Corresponding authors.
E-mail addresses: kakizuka@lif.kyoto-u.ac.jp (A. Kakizuka), kohono@kuhp.kyoto-u.ac.jp (K. Ono).
[1] These authors contributed equally to this work.

https://doi.org/10.1016/j.biopha.2023.115850
Received 24 August 2023; Received in revised form 26 October 2023; Accepted 5 November 2023
Available online 12 December 2023

as the elderly population.

Because the heart has a very high energy demand, it must continuously produce large amounts of ATP to maintain its function [2]. The heart accomplishes this by metabolizing various fuels (fatty acids, glucose, lactate, ketone bodies, pyruvate, amino acids, etc.), primarily through oxidative phosphorylation in the mitochondria. Because this process requires a large amount of oxygen, the heart consumes more oxygen per unit weight than any other organ in the body. Therefore, any disruption in the energy metabolism pathways that produce ATP or the oxygen supply to the heart can have devastating effects on cardiac muscles and functions. Moreover, HF itself is known to alter cardiac energy metabolism, insidiously leading to more severe HF [3].

Pharmacological targeting of energy metabolic pathways is an emerging therapeutic approach to increase cardiac energy efficiency, eliminate energy deficit, and improve cardiac function in failing hearts. Current methods being attempted include ketone body oxidation [4], glycolytic hyperglycemia [5], fatty acid oxidation [6] and increased oxidation of branched-chain amino acids [7]. However, strategies to maintain ATP levels by reducing ATP consumption have never been clinically attempted or even devised [8].

Valosin-containing protein (VCP) is a member of the ATPase family associated with diverse cellular activities (AAA) and is abundantly expressed in all cells. Accordingly, in addition to its function as an ATPase, VCP has been reported to be involved in a variety of cellular functions, including proteasome-mediated proteolysis, endoplasmic reticulum (ER)-associated degradation, lysosomal proteolysis, autophagy, cell cycle progression, and membrane fusion [9]. Recently, toxic gain-of-function mutations in VCP have been reported to cause inclusion body myopathy associated with Paget's disease of bone and frontotemporal dementia (IBMPFD) [10], and mutations in VCP that cause IBMPFD result in increased ATPase activities [11]. The main clinical phenotypes of IBMPFD are myopathy, bone lesions, and dementia; however, in some IBMPFD patients, cardiac phenotypes such as dilated cardiomyopathy also appear [12].

Kyoto University Substance 121 (KUS121) was developed to selectively inhibit the ATPase activity of VCP without affecting its other cellular functions [13]. In fact, KUS121 has been shown to maintain cellular ATP levels, reduce ER stress, and prevent cell death in vitro without showing any toxicity [13]. We reported previously that KUS121 preserved ATP levels and mitochondrial function in H9C2 rat cardiomyocyte cells after tunicamycin treatment. Furthermore, in murine and porcine ischemia reperfusion injury models, KUS121 ameliorated cardiac damage and preserved cardiac function [14]. Considering the cardiac phenotype of IBMPFD patients and the cytoprotective effect of KUS121 in vivo, we predicted that KUS121 might be effective in the treatment of heart failure.

In this study, we investigated the effects of KUS121 at the cellular level, in a mouse heart failure model, and in a canine heart failure model.

2. Methods

Detailed experimental methods are described in the Supplementary Material section.

2.1. Animals

All animal experiments were approved by the Animal Research Committee, Graduate School of Medicine, Kyoto University (MedKyo23515), and were conducted in accordance with the Guide for the Care and Use of Laboratory Animals (National Academies Press, 2011).

ICR mice were purchased from Charles River Laboratory. Mice were maintained in temperature-controlled rooms with a 14:10 h light:dark cycle in specific pathogen-free conditions at the Institute of Laboratory Animals of Kyoto University Graduate School of Medicine. Beagle dogs were purchased from Kitayama Labs Co., Ltd. and bred at the Shiga Research Laboratory of Nissei Bailis Co. At the end of each experiment, mice and dogs were euthanized by removing their hearts after anesthesia with the anesthetic used during surgery and catheterization, respectively.

2.2. Cell culture experiments

H9C2 rat cardiomyocyte cells were cultured in Dulbecco's modified Eagle's medium (1% glucose; Nacalai Tesque, 08459–64) supplemented with 10% fetal bovine serum and antibiotics (penicillin-streptomycin-glutamine; Gibco™, 10378016). In the in vitro experiments on cardiac hypertrophy, H9C2 cells were serum-starved overnight and then treated with vehicle (dimethyl sulfoxide [DMSO]) or isoproterenol (Sigma Aldrich, I6504) (50–100 μM) in the presence or absence of KUS121 at the indicated concentrations for 24 h. H9C2 cells were fixed in 4% paraformaldehyde at room temperature for 30 min and then washed 3 times in phosphate-buffered saline (PBS). After staining with Phalloidin-iFluor 488 Reagent (Abcam, ab176753) and 4',6-diamidino-2-phenylindole (DAPI; Dojindo, D523), images were captured using an Axio Observer7 inverted microscope system (Zeiss). Cell size measurement was performed using ImageJ64 software (NIH).

2.3. Adult mouse cardiomyocyte (AMCM) isolation and primary culture

Primary cultures of AMCMs were established in accordance with previous reports [15]. The thoracic cavity of anesthetized 8-week-old mice was opened, the descending aorta and inferior vena cava of the heart were excised, and the heart was washed with EDTA buffer. The heart was removed by clamping the ascending aorta with forceps and transferred to a 60-mm dish; EDTA buffer, perfusion buffer, and collagenase buffer were infused until completely absorbed, and the myocardial tissue was perfused. Next, 30–40 mL of collagenase buffer was injected, the clamp was removed, and tissue was harvested from the left ventricle. The tissue was divided into 1 mm^2 pieces, stop buffer was added, and cardiomyocytes were sedimented and isolated while the calcium concentration was returned to physiological extracellular levels. Cardiomyocytes were plated at 30,000–80,000 cells per well in 96-well plates precoated with mouse laminin solution (Gibco™, 23017015, washed after 1 h with PBS, and incubated with M199 medium (Sigma-Aldrich, M4530).

2.4. Pressure-overload cardiac hypertrophy/heart failure model

Transverse aortic constriction (TAC) was performed as described previously [16]. Briefly, 8- to 10-week-old mice were anesthetized with anesthetic (0.3 mg/kg, medetomidine (DOMITOR®, NIPPON ZENYAKU KOGYO Co.,Ltd.), 4·0 mg/kg midazolam (SANDOZ), and 5·0 mg/kg butorphanol (Meiji Animal Health Co., Ltd.)) administered intraperitoneally, and the proximal portion of the sternum was cut open to visualize the aorta. A 7–0 silk suture was placed around the aortic arch distal to the brachiocephalic artery. The suture was tightened firmly around a blunt 26-gauge needle placed adjacent to the aorta. The needle was then removed, and the chest and overlying skin were closed. Sham-operated mice underwent an identical surgical procedure without ligation of the aortic arch. At the end of the operation, 0·3 mg/kg of atipamezole (ANTISEDAN ®, NIPPON ZENYAKU KOGYO Co.,Ltd.) was administered subcutaneously to reverse the medetomidine.

2.5. Pacing-induced canine heart failure model

After induction of general anesthesia with thiopental sodium (20 mg/kg, i.v.: 0·5 g of Labonal injection, Nipro ES Pharma Corporation) in 10- to 12-month-old male beagle dogs (9·80–11·50 kg), a tracheal cannula was inserted into the airway, and artificial respiration was performed with an Acoma veterinary ventilator (PRO-45Va, Acoma Medical Corporation). Anesthesia was maintained by inhalation of a gas

mixture (Air: O_2 = 3: 0·2) and 1·0–2·5% isoflurane (isoflurane inhalation solution [Pfizer], Mylan Seiyaku Co., Lid.) using an Acoma animal anesthesia machine (NS-5000A, Acoma Medical Industry Co., Ltd.) to maintain a constant depth of anesthesia. After local anesthesia with lidocaine, an incision was made in the right side of the neck of the animal, and an animal intravital cardiac pacemaker (SIP-501, Star Medical Corporation) was implanted under X-ray guidance (BV Pulsera, Philips). Pacing was started at 244–251 beats/min on postoperative day 1. Dogs with EF decreasing to 30–50% at 4 weeks after pacemaker activation were subjected to analysis.

2.6. Statistical analysis

Measurements are presented as means ± standard error of the mean (SEM). For other statistical comparisons, unpaired Student's *t*-test (two groups, parametric), Mann–Whitney test (two groups, non-parametric), or one-way analysis of variance (ANOVA) with Bonferroni's post hoc test (three or more groups) were used as indicated in the figure legends. A p-value of $< 0{\cdot}05$ was considered as statistically significant. Statistical analyses were performed using GraphPad Prism 7 (GraphPad Software, Inc.).

3. Results

3.1. Analyses of immediate effects of KUS121 on pressure overload-induced heart failure in mice

KUS121 preserves cardiac ATP levels after ischemia-reperfusion, reduces myocardial infarct size, and improves cardiac function [16]. During the analyses, we noticed that KUS121 appeared to enhance contraction of the heart immediately. Thus, KUS121 would likely be able to improve reduced cardiac function in heart failure. After determining the dose in preliminary experiments (Supplementary Figure 1), KUS121 was administered intraperitoneally at 50 mg/kg to mice with reduced cardiac function after 8 weeks of TAC, and cardiac function was analyzed by echocardiography before and 10 min after administration. As expected, the LVEF was significantly increased, but the LVDd was decreased by KUS121 administration (Supplementary Movie, Fig. 1a and b). Unexpectedly, the heart rate (HR) did not increase, or stayed within the normal range after KUS121 administration (Fig. 1c). Next, we measured the creatine phosphate (PCr) /ATP ratio in the heart. The region of interest for measuring the ^{31}P-MR spectrum of the left ventricular anterior wall and its ^{1}H-MR image are shown in Fig. 1d. Fig. 1e shows the representative spectra of myocardial energetics measured by ^{31}P-MR spectroscopy before and 10 min after KUS121 administration (50 mg/kg) in mice 5 weeks after TAC. KUS121 significantly increased the PCr/βATP ratios and PCr/γATP ratios (Figs. 1f and 1g). Although SGLT2 inhibitors have also been shown to increase myocardial ATP production associated with increased ketones, KUS121 treatment did not increase urine output. (Supplementary Figure. 2). Next, to analyze the comprehensive metabolite changes in the heart, metabolomics analysis was performed in sham and TAC hearts with or without KUS121. Metabolomics analyses showed no obvious changes in fatty acid metabolism or the TCA cycle (Supplementary Figs. 3a and 3b). These results indicate that KUS121 promptly increases cardiac ATP levels within 10 min after administration and improves left ventricular contractility with no apparent metabolic change or increase of HR.

3.2. KUS121 effects on acute heart failure

Next, to examine the efficacy of KUS121 for acute uncompensated pressure overload, and whether it can be used for acute heart failure, we tested the protocol shown in Fig. 2a using the heart immediately after TAC. In this experiment, 50 mg/kg of KUS121 or 5% Tz (glucose) was administered intraperitoneally at the same time as the transverse aorta was constricted, and the results were analyzed 3 h later. It is known that immediately after TAC, there is an increase in lung weight and a transient increase in LVEDP [17], which was used as a model for the pathogenesis of acute pressure overload-induced heart failure [18].

As a result, there was no effect on heart weight (HW) per body weight (HW/BW) (Fig. 2b). On the other hand, the lung weight per body weight was increased by TAC, and KUS121 appeared to completely prevent the increase (Fig. 2c). In addition, brain natriuretic peptide (BNP) mRNA expression in the heart was increased by TAC, but its increase was suppressed by KUS121 (Fig. 2d). KUS121 improved LVEF, ascertained by echocardiography 3 h after TAC (Fig. 2e). These results suggest that KUS 121 has a positive impact on acute heart failure.

3.3. In vivo effects of KUS121 on hemodynamics in a canine heart failure model with high-frequency right ventricular pacing

Since we have found that KUS121 has a therapeutic effect when administered during chronic heart failure in mice, we next evaluated its detailed hemodynamic effects in a canine heart failure model. In this model, high-frequency right ventricular pacing (240–250/min) was performed for 4 weeks, which leads to severe systolic dysfunction [19]. The HR decreased after the 15 min administration at 40 mg/h (i.e., 45 min after initiation of KUS121 administration), but there was no significant change in systolic blood pressure in this setting (Fig. 3b and c). In contrast, mean pulmonary artery (mPA) pressure decreased after the 15 min administration at 40 mg/h, and left ventricular end-diastolic pressure (LVEDP) significantly decreased after the 15 min administration at 20 mg/h and 40 mg/h (Fig. 3d and e). On the other hand, adjusted left ventricular dp/dt (dp/dt divided by LVEDP) significantly increased after the 15 min administration at 20 mg/h and 40 mg/h, and pulmonary artery vascular resistance (PVR) decreased after the 15 min administration at 40 mg/h (Fig. 3f and g). Next, end-systolic pressure-volume relation (ESPVR) and end-diastolic pressure-volume relation (EDPVR) were measured by PV-loop analysis during occlusion tests ((Fig. 3h (before administration) and Fig. 3i (after the 15 min administration at 40 mg/h). ESPVR and EDPVR are shown in red and blue, respectively). Comparing the baseline and the line after the 15 min administration at 40 mg/h, ESPVR showed an increasing trend and EDPVR showed a decreasing trend (Fig. 3j and k). In addition, LVEF in echocardiography was significantly increased by the 40 mg/h administration (Fig. 3l). These results indicate that KUS121 improves left ventricular contractility and improves indices of congestion in a heart failure model in medium-sized animals promptly after administration, without increasing HR.

3.4. KUS121 attenuates hypertrophy and reduces ER stress, which are induced by isoproterenol, in H9C2 cardiomyocytes

To further investigate the cardioprotective effect against cardiac hypertrophic stimuli, H9C2 cells were treated with KUS121 and/or isoproterenol. As shown in Supplementary Figures 4a and 4b, treatment with 50 μM isoproterenol for 24 h significantly increased the cell area of H9C2 cells, and the addition of 50 μM KUS121 reversed the isoproterenol-mediated increase in cell area, which was comparable to non-treated cells (far left column). Moreover, 100 μM isoproterenol decreased intracellular ATP levels, whereas the concomitant addition of KUS121 prevented the decrease (Supplementary Fig. 4c). Furthermore, 100 μM isoproterenol increased BNP mRNA expression, whereas co-treatment with KUS121 prevented the increase of BNP mRNA expression in a dose-dependent manner (Supplementary Fig. 4d). Recent studies have revealed that UPR and ER-induced apoptosis is involved in the pathophysiology of various cardiovascular diseases, including heart failure [20]. Therefore, effects on ER stress were examined: 100 μM isoproterenol increased CHOP mRNA expression, but co-treatment with high doses of KUS121 (50 and 75 μM) decreased its level significantly (Supplementary Fig. 4e). Consistently, 100 μM isoproterenol increased the abundance of CHOP protein, and co-treatment with 50 μM

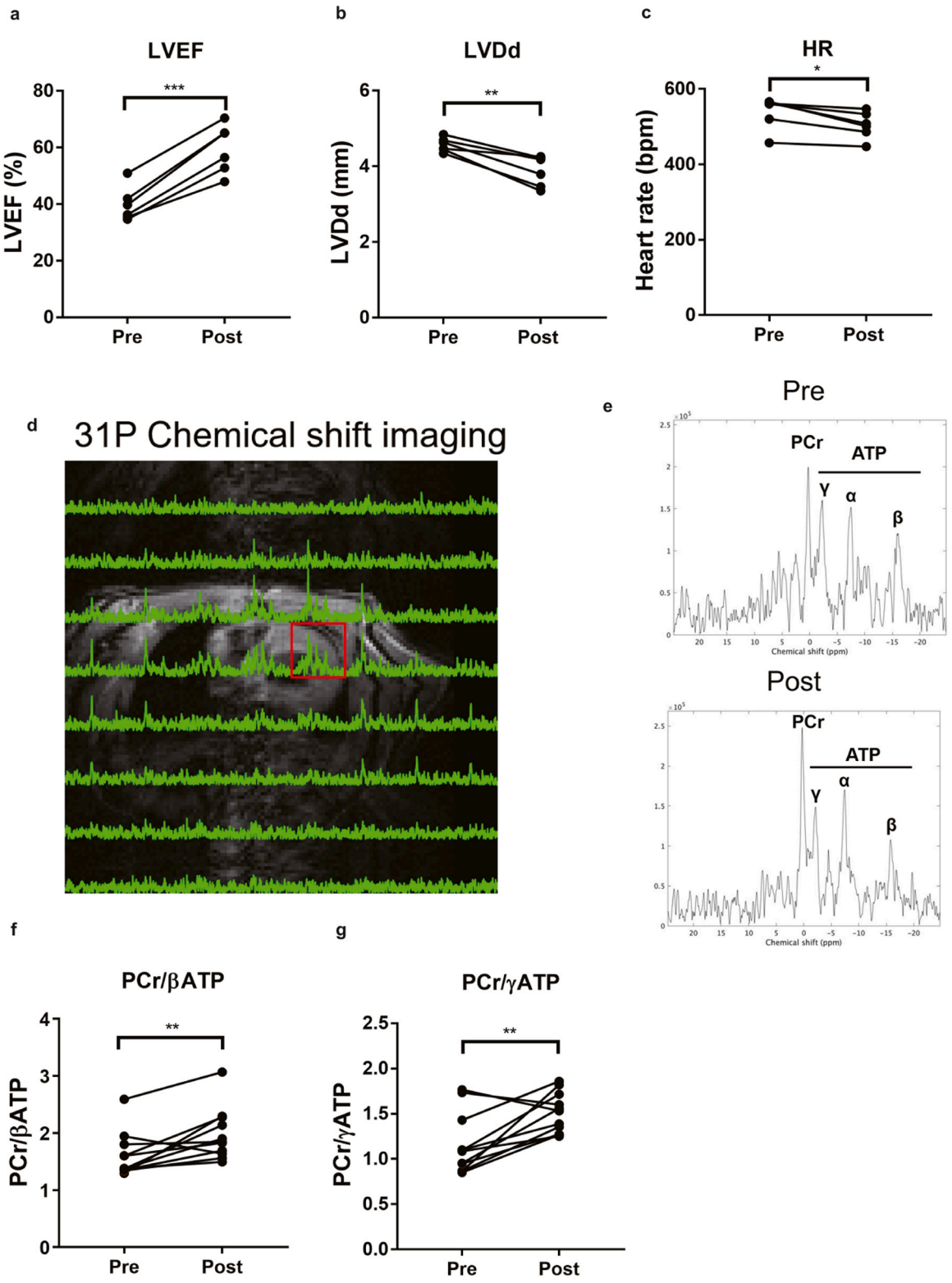

Fig. 1. Analysis of acute effects of KUS121 on pressure overload induced heart failure in mice. (a-c) Changes in left ventricular ejection fraction (LVEF) (a), left ventricle end-diastolic diameter (LVDd) (b), and heart rate (HR) (c) assessed by echocardiography before (Pre) and 10 min after (Post) KUS121 injection (50 mg/kg) in mice 8 weeks after TAC surgery that was performed at 8 weeks of age. n = 6. (d-g) Assessment of myocardial energetics using ^{31}P-magnetic resonance (MR) spectroscopy. (d) ^{1}H MR image to define the region of interest to measure a ^{31}P MR spectrum of the LV anterior wall (red square). (e) Representative spectra of myocardial energetics measured by ^{31}P-MR spectroscopy before (Pre) and 10 min after (Post) KUS121 injection (50 mg/kg) in mice 5 weeks after TAC surgery that was performed at 8 weeks of age (f) PCr/βATP ratios and (g) PCr/γATP ratios in left ventricles of mice subjected to TAC, assessed before (Pre) and 10 min after (Post) KUS121 injection (50 mg/kg) in mice 5 weeks after TAC surgery that was performed at 8 weeks of age. n = 11. * , $p < 0{\cdot}05$; * *, $p < 0{\cdot}01$.

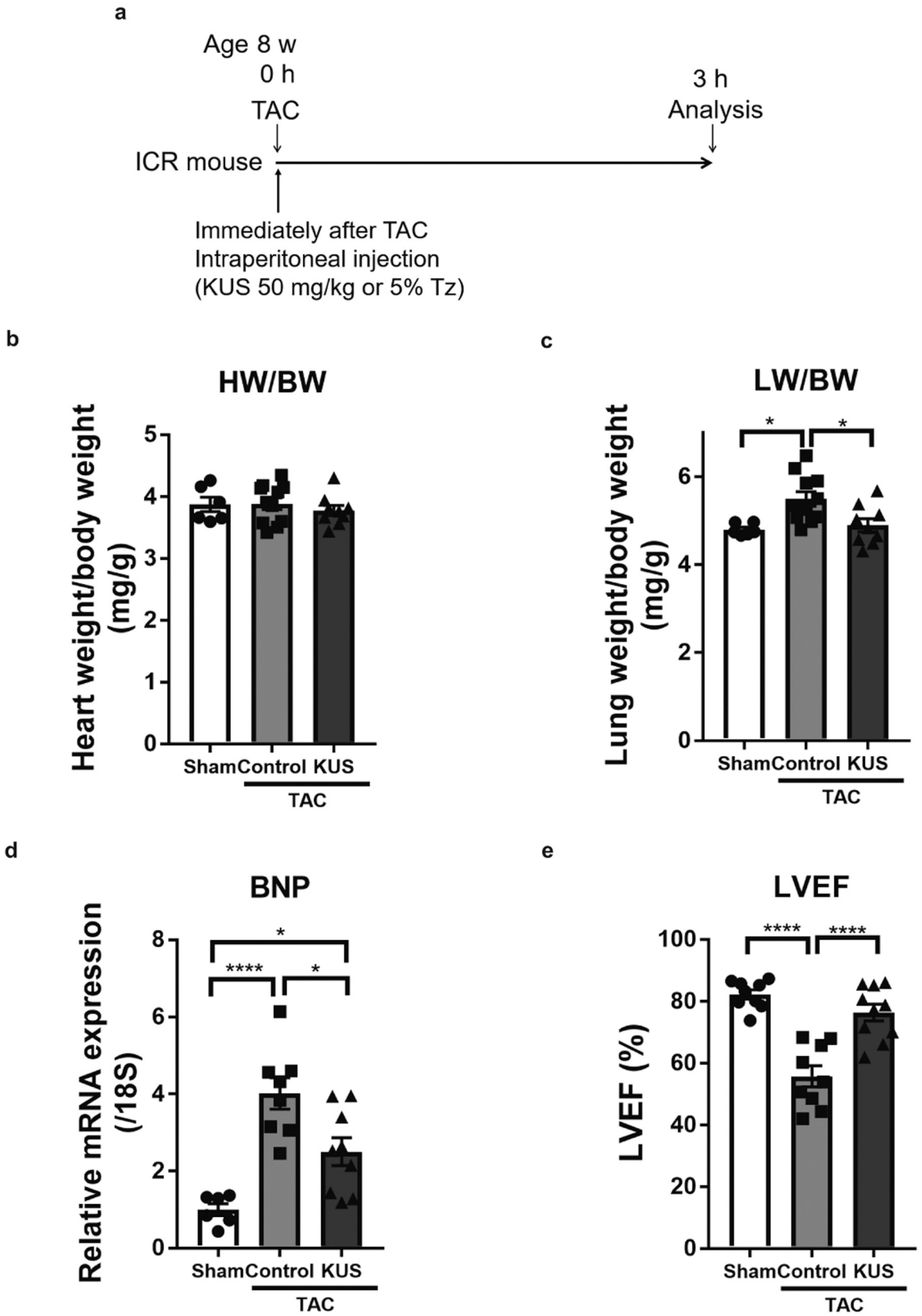

Fig. 2. Analysis of the pharmacokinetics of KUS121 and its effect on acute heart failure. (a) Schematic diagram showing the experimental protocol for KUS121 or 5% Tz injection to pressure overload induced acute heart failure mice. TAC: transverse aortic constriction. Tz: glucose. (b) Ratio of heart weight to body weight and (c) lung weight to body weight of sham, 5% Tz injected mice subjected to TAC, and KUS121 (50 mg/kg) injected mice subjected to TAC. n = 6–11. (d) mRNA levels of BNP. n = 6–9. (e) Left ventricular ejection fraction (LVEF) assessed by echocardiography 3 h after TAC. n = 6–9. * , $p < 0{\cdot}05$; * ** *, $p < 0{\cdot}0001$.

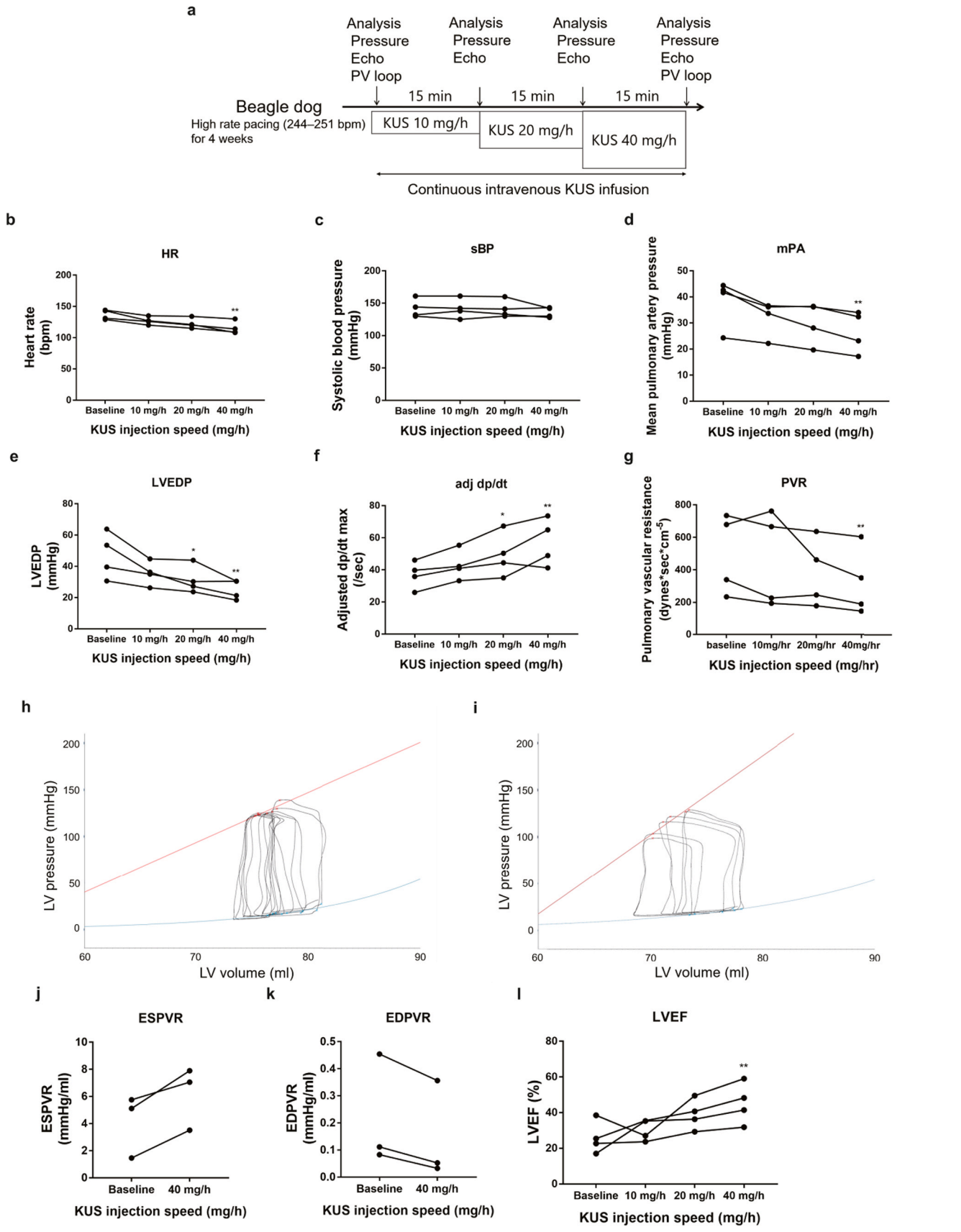

(caption on next page)

Fig. 3. Analysis of effects of KUS121 on hemodynamics in canine heart failure model with high-frequency right ventricular pacing. (a) Schematic diagram showing the experimental protocol of KUS121 injection to treat rapid ventricular pacing induced heart failure in beagle dogs. PV; pressure-volume. (b-h) Serial changes in (b) heart rate (HR), (c) systolic blood pressure (SBP), (d) mean pulmonary artery pressure (mPA), (e) left ventricle end-diastolic pressure (LVEDP), (f) adjusted dp/dt, and (g) pulmonary vascular resistance (PVR) to different KUS121 injection speeds. n = 4. (h, i) Representative PV loop shift by preload reductions through an inferior vena cava occlusion at (j) baseline and (k) during KUS121 injection (40 mg/h). (l) Changes from baseline in the end-systolic PV relationship (ESPVR) obtained by PV loop shift during KUS121 injection (40 mg/h) from baseline. n = 3. (m) Changes from baseline in the end-diastolic pressure-volume relationship (EDPVR) obtained by PV loop shift during KUS121 injection (40 mg/h). n = 3. (n) Changes due to KUS121 injection speed in left ventricular ejection fraction (LVEF) assessed by echocardiography, compared with baseline. n = 4. * , $p < 0{\cdot}05$; **, $p < 0{\cdot}01$.

KUS121prevented the increase (Supplementary Fig. 4f). Protein levels of another ER stress marker, inositol-requiring enzyme 1α (IRE1α), also tended to be attenuated by KUS121 (Supplementary Fig. 4g). However, this is a non-significant trend. Also suggestive, phosphorylation of IRE1-α tended to normalize with KUS121 treatment. In light of previous reports, collectively, these results suggest that KUS121 suppresses multiple pathways of ER stress [21].

3.5. KUS121 attenuates cardiac hypertrophy, heart failure which is induced by TAC

Since the cytoprotective effects of KUS121 on cardiac hypertrophic stimuli were confirmed, we next examined the effects of KUS121 in mice from immediately after TAC to the cardiac hypertrophic phase. After TAC, 50 mg/kg KUS121 or 5% Tz was administered intraperitoneally once daily, and the mice were analyzed 14 days later (Fig. 4a). KUS121 administration significantly prevented the increases of both HW and HW/BW (Supplementary Fig. 5a and Fig. 5b). Histological analysis showed that the increase in cell cross-sectional area induced by TAC was significantly inhibited by KUS121, consistent with the H9C2 experiments (Figs. 4c, and 4d and Supplementary Fig. 5b). Furthermore, in echocardiographic analyses, intraventricular septal thickness in diastole (IVSd) and LV mass were increased by TAC, and KUS121 significantly attenuated the increases (Supplementary Figs. 5c and 5d). KUS121 significantly ameliorated the TAC-induced decrease in LVEF. (Fig. 4e). These results indicated that daily administration of KUS121 can suppress cardiac hypertrophy and prevent deterioration of the cardiac function in the TAC model.

Since KUS121 was found to inhibit cardiac hypertrophy, we wondered if it could also ameliorate fibrosis, so we investigated the effect of KUS121 once the heart failure had progressed to fibrosis. Moreover, we investigated the effects of multidose KUS121 administration on an in vivo heart failure model in mice. After confirming a decrease in LVEF 5 weeks after TAC, 50 mg/kg KUS121 or 5% Tz was administered intraperitoneally once daily for an additional 3 weeks (8 weeks post TAC) (Fig. 4f). Administration of KUS121 significantly reduced the increase in HW/BW (Supplementary Fig. 6a). The ratio of lung weight to body weight increased with TAC, and KUS121 marginally prevented the increase (Supplementary Fig. 6b). The expression of Col1a1 and Postn, indicators of fibrosis, was significantly suppressed by KUS121. (Supplementary Fig. 6c and Fig. 4g). Histological analysis showed that the area of fibrosis (blue colored area by Masson trichrome staining) was reduced by KUS121 treatment (Figs. 4h and 4i). Furthermore, echocardiographic analysis at 5 weeks post-TAC showed that IVSd and LVEF increased and decreased, respectively, compared to sham surgery; IVSd continued to increase at 5–8 weeks post-TAC, but KUS121 significantly suppressed the increase (Supplementary Fig. 6d); LVEF continued to decrease at 5–8 weeks post-TAC, but KUS121 significantly inhibited its decrease (Fig. 4j). Taken together, these results indicate that even after the onset of cardiac hypertrophy and deterioration of cardiac function 5 weeks after TAC, administration of KUS121 can reduce or prevent further cardiac hypertrophy and fibrosis and prevent or delay the progressive worsening of cardiac functions.

3.6. AMCMS contractile motion indicates that KUS121 possibly changes contractility by increasing or decreasing intracellular ATP

These results suggest that KUS121 improves cardiac function through a mechanism different from that of conventionally used catecholamines. We compared KUS121 to isoproterenol, the most typical beta-stimulant drug. Also, isoproterenol has been used as a positive control since many experiments have been conducted so far. The motion waveforms of AMCMs before and after isoproterenol or KUS121 stimulation were also measured. For this purpose, high-speed video microscopy with motion vector analysis was used.

Motion waveforms, representing peaks of contraction and relaxation at baseline and after treatment with isoproterenol or KUS121, were calculated from single AMCMs. (Fig. 5a and b). Four parameters related to contractile motion were extracted from the two peak kinetic waveforms before and after isoproterenol or KUS121 stimulation: average deformation distance (ADD), maximum contraction speed (MCS), maximum relaxation speed (MRS), and contraction relaxation time (CRD), before and after isoproterenol or KUS121 stimulation. Isoproterenol and KUS121 significantly increased ADD, MCS, and MRS (Fig. 5c and d). However, KUS121 did not affect CRD. These results indicate that isoproterenol has both positive inotropic and chronotropic effects, while KUS121 has only positive inotropic effects and does not increase heart rate, unlike catecholamines.

Since KUS121 promotes the conservation of intracellular ATP by inhibiting the ATPase activity of VCP, we further explored the possible association between intracellular ATP levels and contractility. To this end, we examined how contractility changes when the amount of intracellular ATP is simply decreased (Fig. 5e). We modified an experimental procedure from a previous report [22] to confirm that the amount of intracellular ATP is decreased by antimycin in a dose-dependent manner; moreover, motion analysis under these conditions showed that MSV and MRV were significantly decreased (Fig. 5f). This is consistent with a previous report showing that a decrease in intracellular ATP content decreases contractility [22,23]. This suggests that fluctuations in ATP utilization may affect cardiac contractility.

3.7. Profiles of the Ca^{2+} transient of adult mouse cardiomyocytes stimulated by isoproterenol and KUS121

Ca^{2+} entering cardiac cells via L-type Ca^{2+} channels control the release of Ca^{2+} from the sarcoplasmic reticulum (SR), leading to cell contraction in the process known as excitation-contraction coupling [24].

The Ca^{2+} transients in AMCMS were then quantitatively measured before and after isoproterenol (100 nM) or KUS121 (50 μM) stimulation. Representative figures are shown below (Figs. 6a and 6b). The time to 50% decay and time to 75% decay were significantly shortened for both drugs (Fig. 6c and d). However, isoproterenol significantly increased the peak amplitude of Ca^{2+} transients compared to baseline conditions; KUS121 did not increase the peak amplitude of Ca^{2+} transients compared to baseline conditions (Fig. 6c and d). These results suggest that KUS121 improves cardiac contractility without mobilizing intracellular Ca^{2+}, and it activates intracellular Ca^{2+} reuptake to the sarcoplasmic reticulum (SR).

Caffeine administration was used to estimate Ca^{2+} in the SR. AMCMs

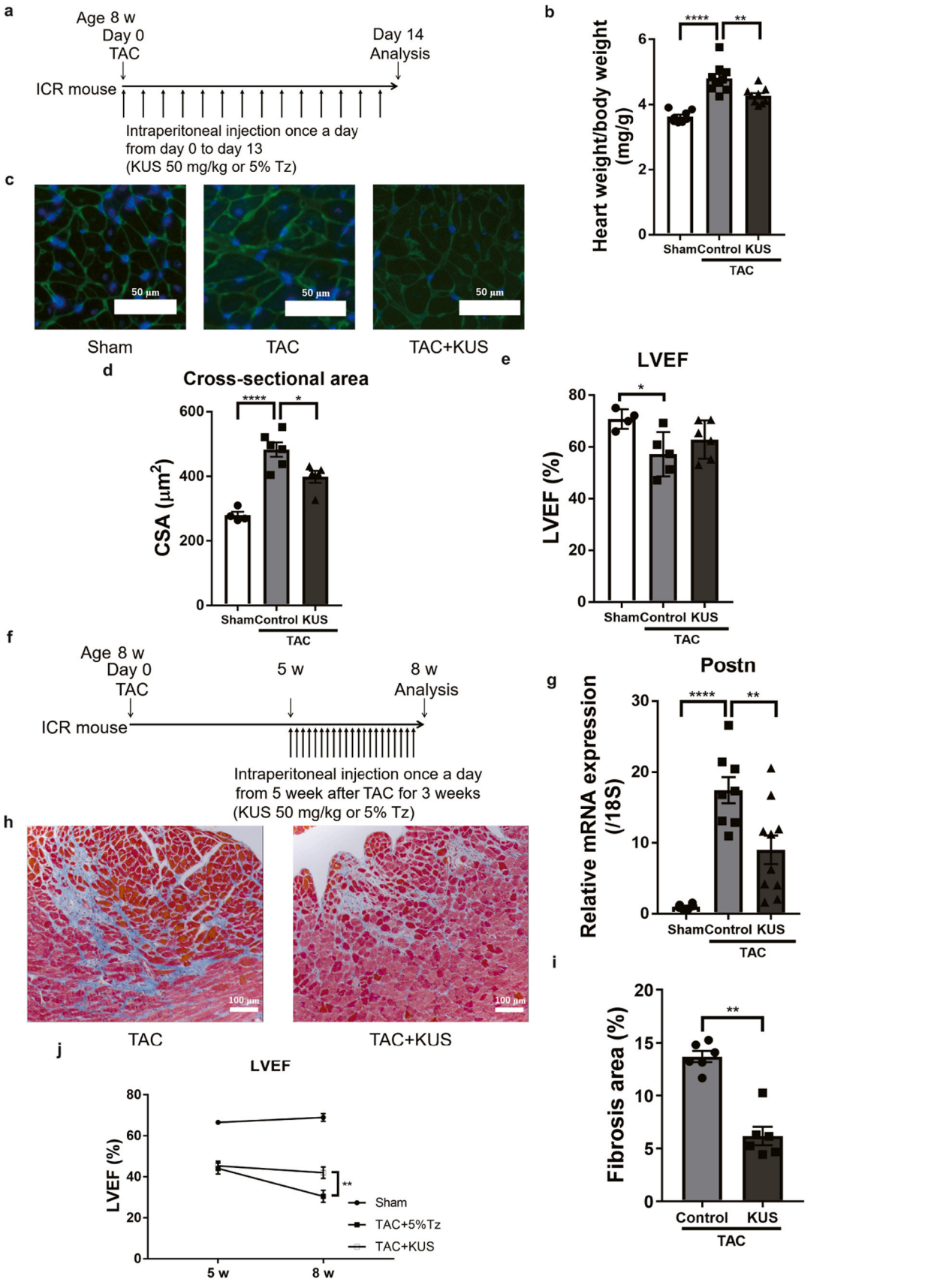

(caption on next page)

Fig. 4. KUS121 attenuates cardiac hypertrophy, heart failure which is induced by TAC. (a) Schematic diagram showing the experimental protocol of KUS121 or 5% Tz injection in mice with pressure overload induced cardiac hypertrophy. TAC: transverse aortic constriction. Tz: glucose. (b) ratio of heart weight to body weight of Sham, 5% Tz injected mice subjected to TAC, and KUS121 (50 mg/kg/day) injected mice subjected to TAC. n = 8–10. (c) Representative images of wheat germ agglutinin (WGA) staining of the heart of Sham, 5% Tz injected mice subjected to TAC, and KUS121 (50 mg/kg/day) injected mice subjected to TAC. Scale bar = 50 μm. (d) Quantification of the cross-sectional area of cardiomyocytes in Sham, 5% Tz injected mice subjected to TAC, and KUS121 (50 mg/kg/day) injected mice subjected to TAC. n = 4–6. (e) Left ventricular ejection fraction (LVEF) assessed by echocardiography. n = 4–6. (f) Schematic diagram showing the experimental protocol for KUS121 or 5% Tz injection in mice with pressure overload induced heart failure. TAC: transverse aortic constriction. Tz: glucose. (g) mRNA levels of Postn. n = 6–10. (h) Representative images of Masson's trichrome staining of the heart of 5% Tz injected mice subjected to TAC, and KUS121 (50 mg/kg/day) injected mice subjected to TAC. Scale bar = 100 μm. (i) Quantification of the fibrosis area. n = 6. (j) Left ventricular ejection fraction (LVEF) changes assessed by echocardiography. n = 6–10. * , $p < 0{\cdot}05$; **, $p < 0{\cdot}01$, *** *, $p < 0{\cdot}0001$.

were stimulated to record systolic Ca^{2+} transients, and SR Ca^{2+} content was quantified after the addition of caffeine. SR Ca^{2+} loading was also quantified indirectly by measuring the amplitude of caffeine induced Ca^{2+} transients. This method assumes that the relationship between cell volume and surface area is unchanged [25–30]. A representative figure is shown (Fig. 6e). As expected, isoproterenol significantly increased the amplitude of the caffeine-induced Ca^{2+} transient, signifying an increased SR Ca^{2+} load (Fig. 6e and f). Interestingly, KUS121 also enhanced the amplitude of caffeine induced Ca^{2+} transients (Fig. 6e and f). This is probably due to the enhancement of SR Ca^{2+} uptake by the supply of ATP, and its effect on Ca^{2+} transients appears to be different from that of isoproterenol.

3.8. KUS121 does not alter signaling molecules downstream of β-adrenergic receptors

We further investigated the difference in the signaling mechanism of KUS121 and β-stimulants. β-stimulants increase intracellular cAMP levels via β-adrenergic receptors [31]. Therefore, we measured intracellular cAMP levels after stimulation with isoproterenol or KUS121. As is well known, isoproterenol stimulation markedly increased intracellular cAMP levels. In contrast, KUS121 stimulation did not increase intracellular cAMP levels (Fig. 7a). Increased cAMP activates protein kinase A (PKA), and activated PKA is known to phosphorylate several proteins including phospholamban (PLB), which is an inhibitor of sarcoplasmic/endoplasmic reticulum calcium ATPase 2a (SERCA2a) [32], and ryanodine receptor 2 (RyR2), leading to the release of Ca^{2+} from the SR/ER into the cell [33].

The actual capacity of SR is determined by the dynamic balance between SR Ca-ATPase, uptake via SERCA2a and release via ryanodine receptors. PLB, a regulatory protein of SERCA, binds to SERCA in its unphosphorylated state and reduces its activity.

We therefore examined PLB and RyR2 phosphorylation after stimulation with isoproterenol or KUS121. Increased phosphorylation of these proteins was observed with isoproterenol but not with KUS121 treatments (Fig. 7b-d). As the Ca^{2+} content of SR increases, the Ca^{2+} available upon release becomes greater; from the behavior of PLB and RyR2, we infer that KUS121 increases Ca^{2+} uptake by providing ATP to SERCA2a without acting on them.

These results clearly demonstrate that KUS121 acts on cardiomyocytes via a mechanism totally different from that of isoproterenol (Supplementary Fig. 7).

4. Discussion

In this study, we first showed that KUS121 dramatically improved cardiac contraction without increasing heart rate; these effects occurred just after the administration of KUS121. Then, in vitro and in vivo therapeutic effects of KUS121 were examined in cardiac hypertrophy and heart failure models. In these experiments, we found that KUS121 can increase the amount of ATP, which is decreased in heart failure, and KUS121 can also increase contractility and improve congestion in vivo. Notably, KUS121 improved not only the contractility of the heart but also its diastolic properties immediately after its administration. Consistent with these results, long-term administration of KUS121 could suppress cardiac hypertrophy and improve myocardial fibrosis. These effects were supported by observations of Ca^{2+} transients and kinetic analysis in primary cardiomyocyte cultures. Initially, we considered that KUS121's actions would partially overlap with those of catecholamines, but KUS121 exerted its effects without increasing HR, and experiments on intracellular signaling indicated that KUS121 acts through a completely different mechanism than catecholamines.

KUS121 was developed to selectively inhibit the ATPase activity of VCP without affecting other cellular functions of VCP. As a result, KUS121 has a positive effect on various diseases by maintaining intracellular ATP levels [34–37]. In our previous study, we demonstrated the effect of KUS121 in reducing myocardial infarction size and improving cardiac function [14]. Those results and the fact that ATP levels in the heart decrease with the progression of heart failure prompted the current experiments reported here.

Our experiments confirmed that immediate and long-term administration of KUS121 compensated for pressure overload without causing cardiac hypertrophy. This increase in EF was consistent with an increase in myocardial PCr/ATP, namely an increase in the myocardial energy source. Furthermore, KUS121 is characterized by its rapid effect in the heart after administration. In a mouse heart failure model, KUS121 was able to improve myocardial contractility within 10 min after administration, suggesting its beneficial use as a therapeutic agent for acute heart failure. In a pacing-induced canine heart failure model, continuous administration of KUS121 reduced mPA, LVEDP, and PVR without increasing HR. The trend of increased ESPVR and improved EF was similar to that observed in the mouse model, while the trend of decreased EDPVR was also observed in the canine model. Thus, these data indicate that KUS121 may provide a favorable therapeutic benefit for acute exacerbations of chronic heart failure.

β-stimulants activate PKA from the direct stimulation of beta receptors, and PKA is known to phosphorylate L-type Ca^{2+} channels and RyR2 [31–33]. As a result, the intracellular Ca^{2+} concentration increases, and myocardial contractility improves. However, cardiac hypertrophy and cardiac fibrosis are inevitable because of enhanced Ca^{2+} signaling [38]. Consequently, β-stimulants are predominantly used to preserve hemodynamics in acute heart failure. In experiments with adult mouse cardiomyocytes, KUS121, in contrast to the adrenergic agonist isoproterenol, increased cardiomyocyte contractility without producing a Ca^{2+} load on cardiomyocytes. This lack of calcium loading may be the reason why KUS121 did not cause cardiac hypertrophy or cardiac fibrosis, but rather reduced them, even after long-term use. It is also possible that KUS121 reduces CHOP protein levels and inhibits cell death that occurs in pressure-overloaded hearts, as shown in in vitro experiments. Thus, it is conceivable that KUS121 could also be used for catecholamine-dependent end-stage heart failure since its mechanism of action is totally different from that of catecholamines. It is also possible that beta receptor downregulation may be eliminated while KUS121 is administered. This possibility still needs to be tested.

Other inotropic agents that differ from catecholamines include Levosimendan. Levosimendan acts quite differently from KUS121; it exerts its inotropic effect by increasing the sensitivity of myocardial troponin C to calcium, and it increases cAMP abundance through PDE-3 inhibition. And it has been suggested that Levosimendan has a risk of arrhythmias and other risks due to the increased cAMP levels [39].

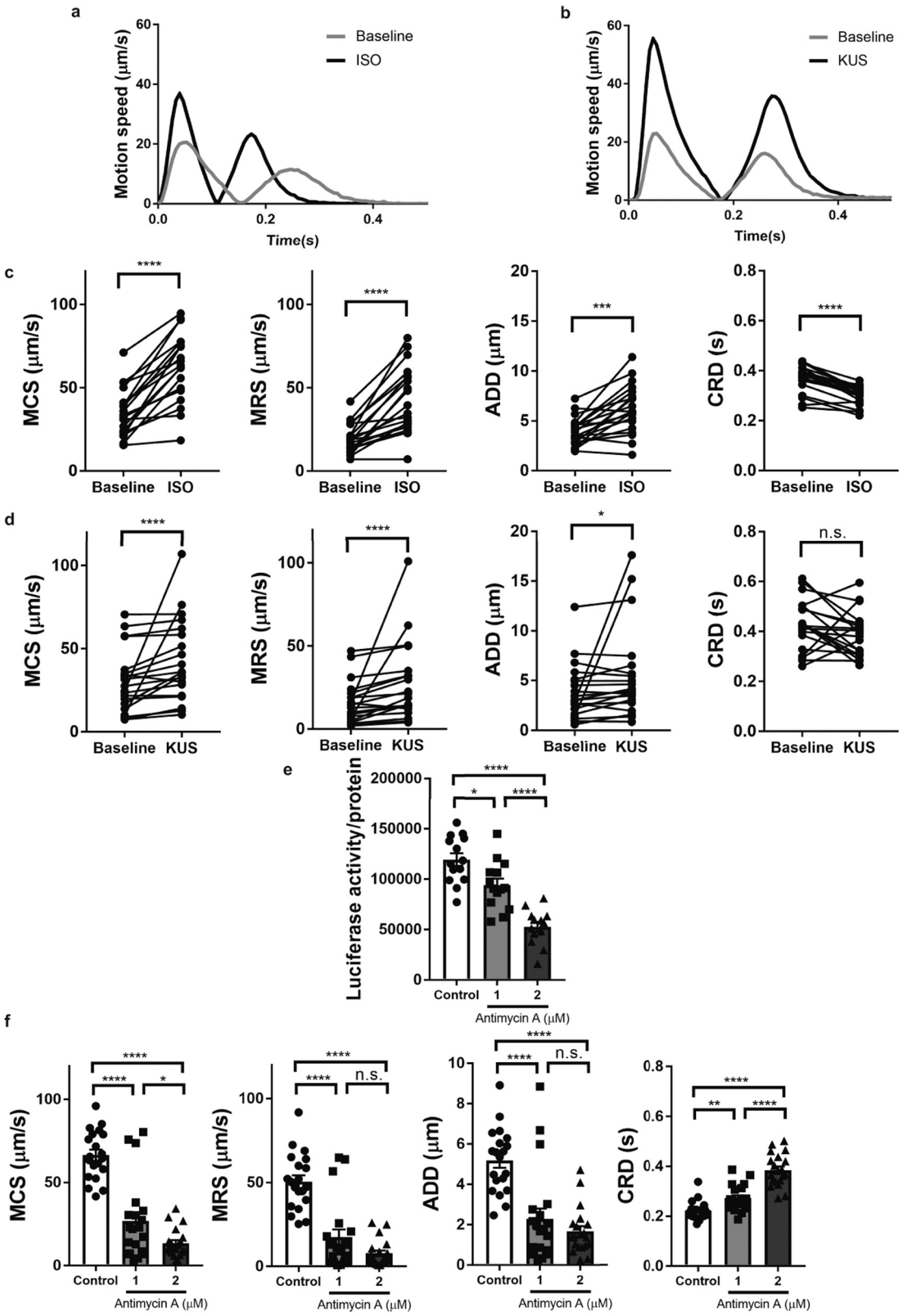

Fig. 5. AMCMs contractile motion indicates that KUS121 possibly changes contractility by increasing or decreasing intracellular ATP. Representative motion waveforms of AMCMs before and after isoproterenol (100 nM) stimulation. (b) Representative motion waveforms of AMCMs before and after KUS121 (50 μM) stimulation. (c) Changes in the contractile parameters, average deformation distance (ADD), maximum contraction speed (MCS), maximum relaxation speed (MRS), and contraction-relaxation duration (CRD) after isoproterenol (100 nM) stimulation. n = 18–20. (d) Changes in the contractile parameters, ADD, MCS, MRS, and CRD after KUS121 (50 μM) stimulation. n = 12. * , $p < 0{\cdot}05$; **, $p < 0{\cdot}01$; *** , $p < 0{\cdot}001$, ****, $p < 0{\cdot}0001$ (e) Decrease in intracellular ATP with antimycin; (AA: inhibitor of mitochondrial electron transfer chain complex III). Cell count corrected for protein concentration. n = 13–14 (f) Changes in the contractile parameters, ADD, MCS, MRS, and CRD. n = 20. * , $p < 0{\cdot}05$; **, $p < 0{\cdot}001$; ****, $p < 0{\cdot}0001$.

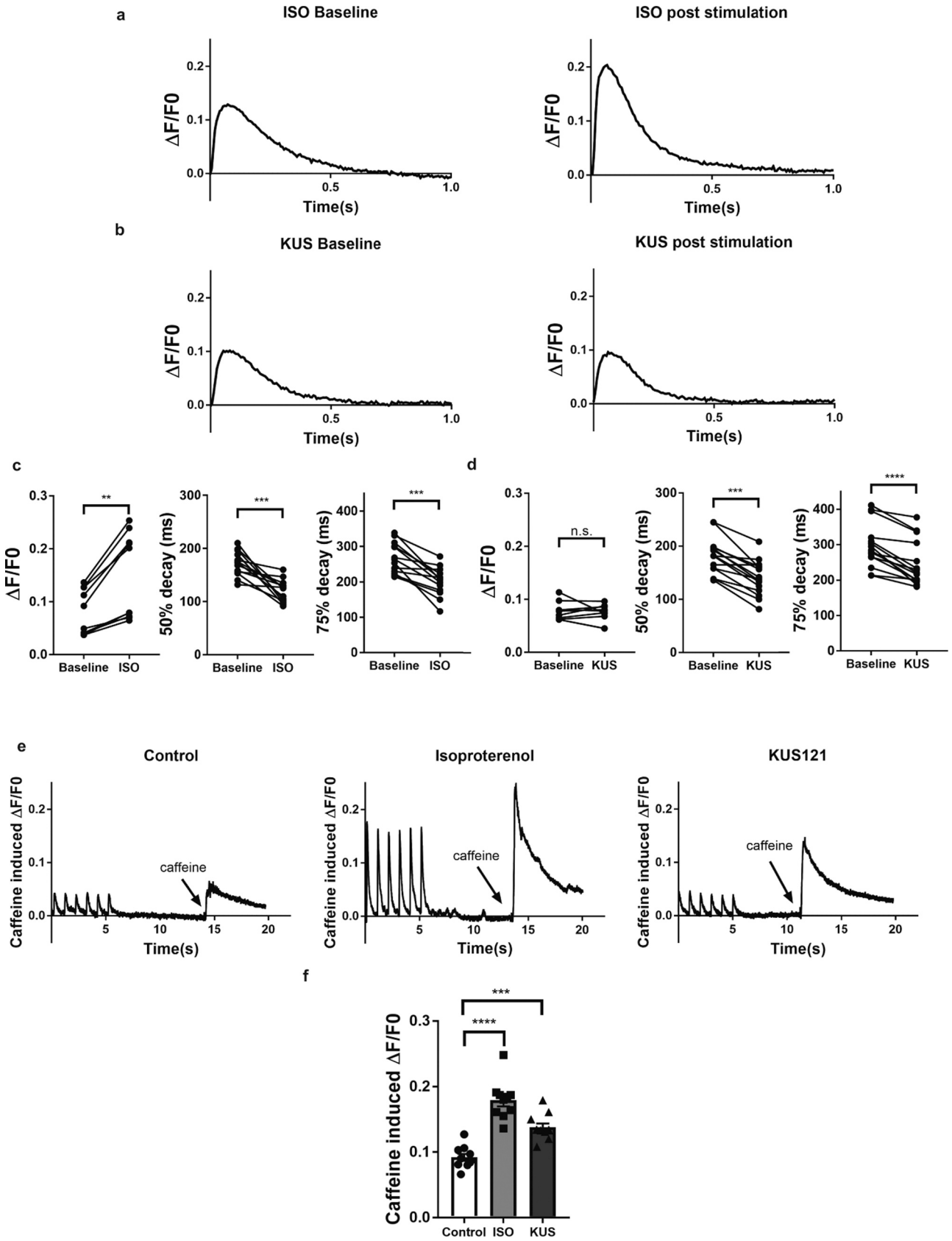

Fig. 6. Profiles of the Ca^{2+} transient of adult mouse cardiomyocytes stimulated by isoproterenol and KUS121. (a) Representative profiles of Ca^{2+} transients in AMCMs before (baseline) and after isoproterenol (100 nM) stimulation. (b) Representative profiles of Ca^{2+} transients in AMCMs before (baseline) and after KUS121 (50 μM). (c) The isoproterenol-induced changes in amplitude, time to 50% decay, and time to 75% decay. n = 14. (d) The KUS121-induced changes in amplitude, time to 50% decay, and time to 75% decay. n = 10. (e) Representative caffeine induced Ca^{2+} transients, (f) The bar charts show the means ± SEM of caffeine induced Ca^{2+} transient amplitude n = 10. * , $p < 0{\cdot}05$; **, $p < 0{\cdot}01$; *** , $p < 0{\cdot}001$; ****, $p < 0{\cdot}0001$.

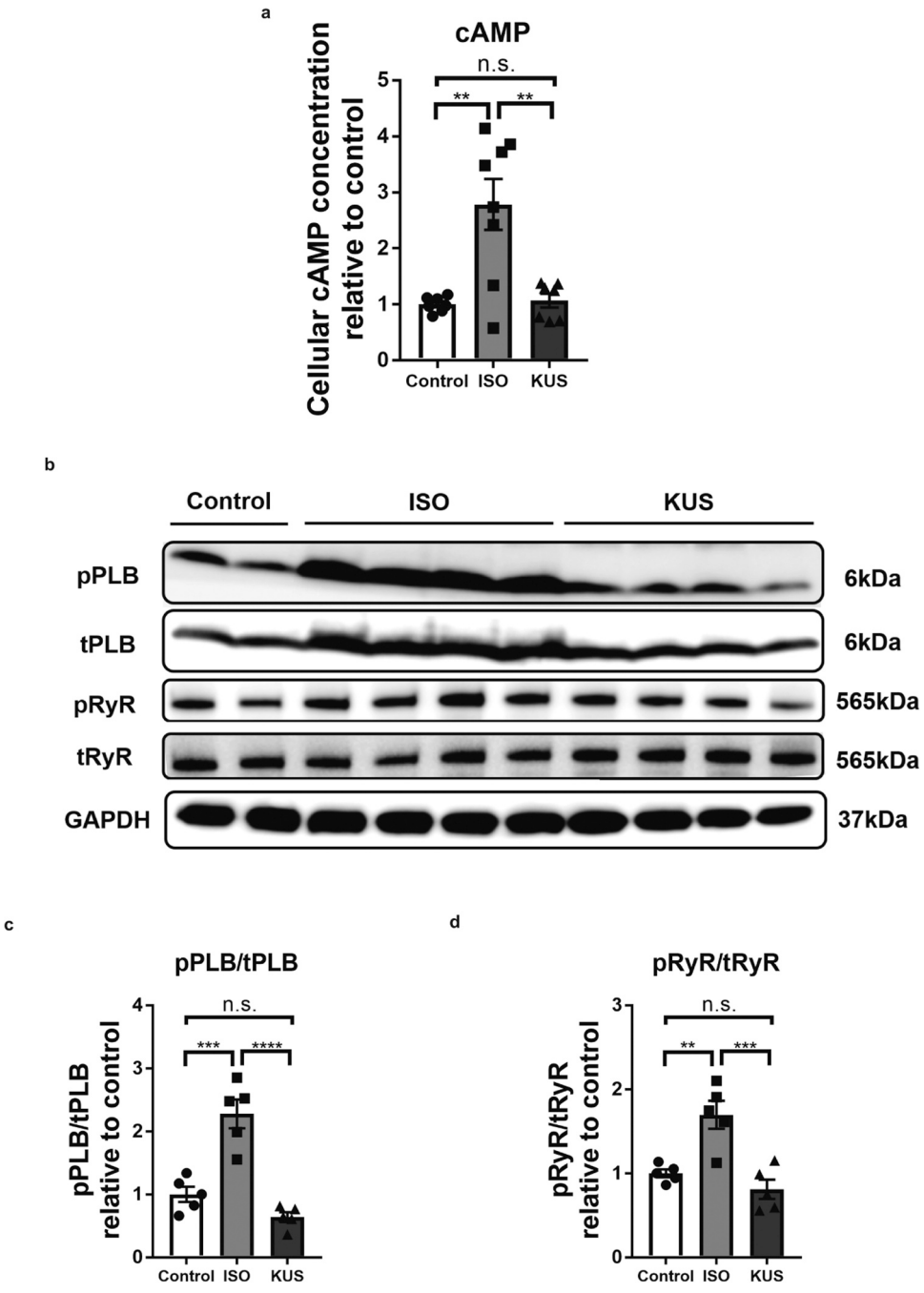

Fig. 7. KUS121 does not alter signaling molecules downstream of β-receptors. (a-d) Adult mouse cardiomyocytes (AMCMs) were isolated and then stimulated by vehicle (DMSO), isoproterenol (100 μM), or KUS121 (100 μM) for 15 min. (a) Measurement of cyclic adenosine monophosphate (cAMP) concentration in AMCMs in each group. n = 7–8. (b) Representative image of western blotting to monitor phospho-phospholamban (pPLB), total-phospholamban (tPLB), phospho-ryanodine receptor (pRyR), total-ryanodine receptor (tRyR), and glyceraldehyde 3-phosphate dehydrogenase (GAPDH) in each group. (c, d) Quantification of western blot results, showing pPLB/tPLB and pRyR/tRyR in each group. n = 5 **, $p < 0.01$; *** , $p < 0.001$; ****, $p < 0.0001$.

Omecamtiv mecarbil, a direct myosin activator, has also been shown to inhibit calcium overload to cardiomyocytes [40]. Based on this promising property, the randomized, placebo-controlled phase 3 Global Approach to Lowering Adverse Cardiac Outcomes Through Improving Contractility in Heart Failure (GALACTIC-HF) trial was conducted. However, add-on omecamtiv mecarbil for heart failure with reduced EF did not reduce cardiovascular death or all-cause mortality [41]. Importantly, we note that KUS121 differs from omecamtiv mecarbil in that it increases the intracellular ATP concentration and also reduces ER stress, acting in a cytoprotective manner, and thus its effects may be even more promising.

SGLT2 inhibitors (SGLT2i) are drugs that lower blood glucose levels by inhibiting glucose reabsorption in the kidneys [42]. The first SGLT2i cardiovascular outcomes trial was the EMPA-REG OUTCOME (Empagliflozin, Cardiovascular Outcomes, and Mortality in Type 2 Diabetes) trial, in which major adverse cardiovascular events (MACE) were significantly reduced, by 14% [43]. Likely modes of action of SGLT2 inhibitors on heart failure include natriuretic and osmotic diuresis, and improvement of myocardial efficiency through increased myocardial ATP production associated with increased ketone bodies. In the present study, we examined whether KUS121 also produces diuretic and metabolic effects and found that KUS121 improves cardiac function through

a different mechanism of action from SGLT2i.

In this study, in addition to the therapeutic effects of KUS121 on heart failure models, we examined its mechanism of action using primary cultured cardiomyocytes, and found that KUS121 does not lead to increased cAMP levels or phosphorylation of PLB and RyR2, which occurs after binding of β agonists, e.g., isoproterenol, to the receptor in the cardiac membrane. Therefore, the effects of KUS121 are most likely due to increased ATP supply to myosin ATPase and SERCA2a (Supplementary Fig. 6).

Based on these results, we propose KUS121 as a novel promising therapeutic agent for heart failure that does not cause cardiac hypertrophy or fibrosis and can be used in both the acute and chronic phases of the disease.

5. Study limitations

In this study, we examined the mechanism using cardiomyocytes from normal hearts, but further experiments using cardiomyocytes in heart failure are needed. For clinical application, the pharmacokinetics and pharmacodynamics of KUS121 and its detailed safety profile need to be confirmed. Once these are confirmed, we can proceed to evaluate the effectiveness of KUS121 in improving heart failure in clinical trials.

6. Conclusions

KUS121 is an agent that maintains intracellular ATP and reduces ER stress. Experimental administration to heart failure models and analysis of intracellular signaling indicate that KUS121 ameliorates cardiac hypertrophy or myocardial fibrosis and may be a novel heart failure therapeutic agent that can be used in both acute and chronic stages of the disease.

Funding

This work was supported by grants from the Ministry of Education, Culture, Sports, Science and Technology and Japan Society for the Promotion of Science KAKENHI; Grant Numbers, 18J20214 (to S.T.), 22K16071 (to S.T.), 20K08904 (to T.H.), 19H03435 (to A.K.), 20H03675 and 20K21600 (to K.O.). Part of this research was funded in collaboration with Kyoto Drug Discovery & Development Co., Ltd.

CRediT authorship contribution statement

KO managed this project. ST and CO designed and performed most in vitro and in vivo experiments and analyzed data. ST, CO, and KO wrote the manuscript. TH, OB, YN and AK provided intellectual input on the project. TH and SW contributed to the canine cardiac catheterization experiments. NS and YI performed in vitro H9C2 experiments. AK and TM helped the experiments of Ca^{2+} transient. HI performed the ^{31}P-MR spectrum. TY, KM, KS helped in vivo experiments. SX, FZ, and EK helped in vitro experiments. KH and TK supported the project financially and discussed the results. AK developed KUS121 and commented on the manuscript.

Declaration of Competing Interest

In relation to this manuscript, Kyoto University has applied for a patent (Tokugan 2021–211106), and S.T., C.O., T.H., S.W., A.K., and K. O. are named as inventors on the patent. The other authors declare no competing interests.

Data Availability

The data underlying this article are available on reasonable request to the corresponding author.

Acknowledgements

None.

Appendix A. Supporting information

Supplementary data associated with this article can be found in the online version at doi:10.1016/j.biopha.2023.115850.

References

[1] K.D. Kochanek, J. Xu, S.L. Murphy, A.M. Minino, H.C. Kung, Deaths: final data for 2009, Natl. Vital.-. Stat. Rep. 60 (2011) 1–116.
[2] G.D. Lopaschuk, J.R. Ussher, C.D. Folmes, J.S. Jaswal, W.C. Stanley, Myocardial fatty acid metabolism in health and disease, Physiol. Rev. 90 (2010) 207–258.
[3] S. Neubauer, The failing heart–an engine out of fuel, N. Engl. J. Med 356 (2007) 1140–1151.
[4] R. Nielsen, N. Moller, L.C. Gormsen, L.P. Tolbod, N.H. Hansson, J. Sorensen, H. J. Harms, J. Frokiaer, H. Eiskjaer, N.R. Jespersen, S. Mellemkjaer, T.R. Lassen, K. Pryds, H.E. Botker, H. Wiggers, Cardiovascular Effects of Treatment with the Ketone Body 3-Hydroxybutyrate in chronic heart failure patients, Circulation 139 (2019) 2129–2141.
[5] B. Liu, A.S. Clanachan, R. Schulz, G.D. Lopaschuk, Cardiac efficiency is improved after ischemia by altering both the source and fate of protons, Circ. Res 79 (1996) 940–948.
[6] W. Wang, L. Zhang, P.K. Battiprolu, A. Fukushima, K. Nguyen, K. Milner, et al., Malonyl CoA decarboxylase inhibition improves cardiac function post-myocardial infarction, JACC Basic Transl. Sci. 4 (2019) 385–400.
[7] T. Li, Z. Zhang, S.C. Kolwicz Jr., L. Abell, N.D. Roe, M. Kim, et al., Defective branched-chain amino acid catabolism disrupts glucose metabolism and sensitizes the heart to ischemia-reperfusion injury, Cell Metab. 25 (2017) 374–385.
[8] D.A. Brown, J.B. Perry, M.E. Allen, H.N. Sabbah, B.L. Stauffer, S.R. Shaikh, et al., Expert consensus document: mitochondrial function as a therapeutic target in heart failure, Nat. Rev. Cardiol. 14 (2017) 238–250.
[9] H. Meyer, C.C. Weihl, The VCP/p97 system at a glance: connecting cellular function to disease pathogenesis, J. Cell Sci. 127 (2014) 3877–3883.
[10] G.D. Watts, J. Wymer, M.J. Kovach, S.G. Mehta, S. Mumm, D. Darvish, et al., Inclusion body myopathy associated with Paget disease of bone and frontotemporal dementia is caused by mutant valosin-containing protein, Nat. Genet 36 (2004) 377–381.
[11] A. Manno, M. Noguchi, J. Fukushi, Y. Motohashi, A. Kakizuka, Enhanced ATPase activities as a primary defect of mutant valosin-containing proteins that cause inclusion body myopathy associated with Paget disease of bone and frontotemporal dementia, Genes Cells 15 (2010) 911–922.
[12] C.U. Hubbers, C.S. Clemen, K. Kesper, A. Boddrich, A. Hofmann, O. Kamarainen, et al., Pathological consequences of VCP mutations on human striated muscle, Brain 130 (2007) 381–393.
[13] H.O. Ikeda, N. Sasaoka, M. Koike, N. Nakano, Y. Muraoka, Y. Toda, et al., Novel VCP modulators mitigate major pathologies of rd10, a mouse model of retinitis pigmentosa, Sci. Rep. 4 (2014), 5970.
[14] Y. Ide, T. Horie, N. Saito, S. Watanabe, C. Otani, Y. Miyasaka, et al., Cardioprotective effects of VCP modulator KUS121 in murine and porcine models of myocardial infarction, JACC Basic Transl. Sci. 4 (2019) 701–714.
[15] M. Ackers-Johnson, P.Y. Li, A.P. Holmes, S.M. O'Brien, D. Pavlovic, R.S. Foo, A simplified, langendorff-free method for concomitant isolation of viable cardiac myocytes and nonmyocytes from the adult mouse heart, Circ. Res 119 (2016) 909–920.
[16] M.O. Date, T. Morita, N. Yamashita, K. Nishida, O. Yamaguchi, Y. Higuchi, et al., The antioxidant N-2-mercaptopropionyl glycine attenuates left ventricular hypertrophy in in vivo murine pressure-overload model, J. Am. Coll. Cardiol. 39 (2002) 907–912.
[17] A. Shirakabe, P. Zhai, Y. Ikeda, T. Saito, Y. Maejima, C.P. Hsu, et al., Drp1-dependent mitochondrial autophagy plays a protective role against pressure overload-induced mitochondrial dysfunction and heart failure, Circulation 29 (133) (2016) 1249–1263.
[18] A. Mebazaa, M. Gheorghiade, I.L. Piña, V.P. Harjola, S.M. Hollenberg, F. Follath, et al., Practical recommendations for prehospital and early in-hospital management of patients presenting with acute heart failure syndromes, Crit. Care Med. 36 (2008) S129–S139.
[19] H.N. Sabbah, C.G. Tocchetti, M. Wang, S. Daya, R.C. Gupta, R.S. Tunin, et al., HNO): a novel approach for the acute treatment of heart failure, Circ. Heart Fail 6 (2013) 1250–1258.
[20] T. Minamino, M. Kitakaze, ER stress in cardiovascular disease, J. Mol. Cell Cardiol. 48 (2010) 1105–1110.
[21] M. Saito, K. Nishitani, H.O. Ikeda, S. Yoshida, S. Iwai, X. Ji, et al., A VCP modulator, KUS121, as a promising therapeutic agent for post-traumatic osteoarthritis, Sci. Rep. (2020 27), 20787.
[22] K. Nakagawa, T. Kishimoto, Unlabeled image analysis-based cell viability assay with intracellular movement monitoring, Biotechniques 66 (2019) 128–133.
[23] D.A. Beard, B. Marzban, O.Y. Li, K.S. Campbell, P.M.L. Janssen, N.C. Chesler, et al., Reduced cardiac muscle power with low ATP simulating heart failure, Biophys. J. 121 (2022) 3213–3223.

[24] M.D. Stern, Theory of excitation-contraction coupling in cardiac muscle, Biophys. J. 63 (1992) 497–517.
[25] J.W. Bassani, R.A. Bassani, D.M. Bers, Relaxation in rabbit and rat cardiac cells: species-dependent differences in cellular mechanisms, J. Physiol. 1994 (476) (1994) 279–293.
[26] M.E. Díaz, H.K. Graham, A.W. Trafford, Enhanced sarcolemmal Ca^{2+} efflux reduces sarcoplasmic reticulum Ca2+ content and systolic Ca2+ in cardiac hypertrophy, Cardiovasc Res 62 (2004) 538–547.
[27] P. Hegner, M. Drzymalski, A. Biedermann, B. Memmel, M. Durczok, M. Wester, et al., SAR296968, a Novel Selective Na+/Ca2+ exchanger inhibitor, improves Ca^{2+} handling and contractile function in human atrial cardiomyocytes, Biomedicines 10 (2022) 1932.
[28] S. Li, A. Chopra, W. Keung, C.W.Y. Chan, K.D. Costa, C.W. Kong, et al., Sarco/endoplasmic reticulum Ca^{2+}-ATPase is a more effective calcium remover than sodium-calcium exchanger in human embryonic stem cell-derived cardiomyocytes, Am. J. Physiol. Heart Circ. Physiol. 317 (2019) H1105–H1115.
[29] S. Lotteau, R. Zhang, A. Hazan, C. Grabar, D. Gonzalez, S. Aynaszyan, et al., Acute genetic ablation of cardiac sodium/calcium exchange in adult mice: implications for cardiomyocyte calcium regulation, cardioprotection, and arrhythmia, J. Am. Heart Assoc. 10 (2021), e019273.
[30] S. Ozdemir, V. Bito, P. Holemans, L. Vinet, J.J. Mercadier, A. Varro, et al., Pharmacological inhibition of na/ca exchange results in increased cellular Ca^{2+} load attributable to the predominance of forward mode block, Circ. Res. 102 (2008) 1398–1405.
[31] J.B. Osnes, I. Oye, Adenosine 3',5'-cyclic monophosphate in perfused rat hearts exposed to isoprenaline and dopamine, Acta Physiol. Scand. 96 (1976) 100–113.
[32] D.H. MacLennan, E.G. Kranias, Phospholamban: a crucial regulator of cardiac contractility, Nat. Rev. Mol. Cell Biol. 4 (2003) 566–577.
[33] S.O. Marx, S. Reiken, Y. Hisamatsu, T. Jayaraman, D. Burkhoff, N. Rosemblit, et al., PKA phosphorylation dissociates FKBP12.6 from the calcium release channel (ryanodine receptor): defective regulation in failing hearts, Cell 101 (2000) 365–376.
[34] H. Kinoshita, T. Maki, K. Yasuda, N. Kishida, N. Sasaoka, Y. Takagi, et al., KUS121, a valosin-containing protein modulator, attenuates ischemic stroke via preventing ATP depletion, Sci. Rep. 9 (2019), 11519.
[35] M. Nakano, H. Imamura, N. Sasaoka, M. Yamamoto, N. Uemura, T. Shudo, et al., ATP maintenance via two types of ATP regulators mitigates pathological phenotypes in mouse models of Parkinson's disease, EBioMedicine 22 (2017) 225–241.
[36] N. Nakano, H.O. Ikeda, T. Hasegawa, Y. Muraoka, S. Iwai, T. Tsuruyama, et al., Neuroprotective effects of VCP modulators in mouse models of glaucoma, Heliyon 2 (2016), e00096.
[37] M. Nishita, S.Y. Park, T. Nishio, K. Kamizaki, Z. Wang, K. Tamada, et al., Ror2 signaling regulates Golgi structure and transport through IFT20 for tumor invasiveness, Sci. Rep. 7 (1) (2017).
[38] J.D. Molkentin, J.R. Lu, C.L. Antos, B. Markham, J. Richardson, J. Robbins, et al., A calcineurin-dependent transcriptional pathway for cardiac hypertrophy, Cell 93 (1998) 215–228.
[39] C. Maack, T. Eschenhagen, N. Hamdani, F.R. Heinzel, A.R. Lyon, D.J. Manstein, et al., Treatments targeting inotropy, Eur. Heart J. 40 (2019) 3626–3644.
[40] F.I. Malik, J.J. Hartman, K.A. Elias, B.P. Morgan, H. Rodriguez, K. Brejc, et al., Cardiac myosin activation: a potential therapeutic approach for systolic heart failure, Science 331 (2011) 1439–1443.
[41] J.R. Teerlink, R. Diaz, G.M. Felker, J.J.V. McMurray, M. Metra, S.D. Solomon, et al., GALACTIC-HF investigators cardiac myosin activation with omecamtiv mecarbil in systolic heart failure, N. Engl. J. Med 384 (2021) 105–116.
[42] C. Clar, J.A. Gill, R. Court, N. Waugh, Systematic review of SGLT2 receptor inhibitors in dual or triple therapy in type 2 diabetes, BMJ Open 2 (2012), e001007.
[43] B. Zinman, C. Wanner, J.M. Lachin, D. Fitchett, E. Bluhmki, S. Hantel, et al., EMPA-REG OUTCOME investigators empagliflozin, cardiovascular outcomes, and mortality in Type 2 diabetes, N. Engl. J. Med. 373 (2015) 2117–2128.